Outdoor UHF RFID: Phase Stabilization for Real-World Applications

Mathieu Le Breton, Laurent Baillet, Éric Larose, Etienne Rey, Philippe Benech, Denis Jongmans, Fabrice Guyoton

Outdoor UHF RFID: Phase Stabilization for Real-World Applications

Mathieu Le Breton, Laurent Baillet, Eric Larose, Etienne Rey,
Philippe Benech, Denis Jongmans, and Fabrice Guyoton

This paper investigates meteorological factors that affect the phase of radio-frequency identification (RFID) passive tags at 868 MHz, in outdoor conditions. The study identifies the effect of water on the tag and base antennas, the effect of tem-perature on the cables, tags, and base antenna, the effect of the tag support moisture, and the effect of atmospheric conditions on wave velocity. Combined, these effects could lead to over 8.1 radi-ans phase drift over a year, in a typical environment. In a tag location tracking application, that would correspond to an error of 22 cm. This paper proposes techniques to correct these effects and to increase the phase stability. These techniques are applied to a new RFID system, which is tested in outdoor conditions, for five months. The new system improves the phase stability for rainy days, dry days, and long-term drift by a factor of 3, 12, and 5, respectively. After corrections, the long-term drift was reduced to below 0.05 radians per month, which corresponds to 1.5 millimeter per month.

Keywords—RFID, localization, continuous wave, phase, outdoor, meteorological factors.

I. Introduction

BACKSCATTER tag radio-frequency identification (RFID) techniques [1] have considerably developed in the last decade, by adding location tracking [2] and environment sensing [3] capabilities.

We aim to track low-cost tag location for monitoring the stability of structures prone to slow motions, such as landslides, volcanoes, and civil infrastructures. Those structures typically move from a few centimeters to a few meters over a year, requiring an accuracy of ten centimeters or less per year. There are already solutions on the market, such as GPS [4], optical laser [5], photogrammetry [6], radar interferometers [7], or radar nodes [8]. However, passive RFID tags offer a lower-cost alternative in terms of installation and maintenance. Real-time monitoring of tag grids would provide dense data, both in space and time, at reasonable cost.

M. Le Breton is with ISTerre, CNRS, Université Grenoble Alpes, F-38000 Grenoble, France, and also with Géolithe, 38920 Crolles, France (e-mail: mathieu.le-breton@univ-grenoble-alpes.fr).

L. Baillet, E. Larose, and D. Jongmans are with ISTerre, CNRS, Université Grenoble Alpes, F-38000 Grenoble, France (e-mail: laurent.baillet@univ-grenoble-alpes.fr; eric.larose@univ-grenoble-alpes.fr; denis.jongmans@univ-grenoble-alpes.fr).

E. Rey and F. Guyoton are with Géolithe, 38920 Crolles, France (e-mail: etienne.rey@geolithe.com; fabrice.guyoton@geolithe.com).

P. Benech is with the Institute of Microelectronics, Electromagnetic and Photonics, MINATEC, 38016 Grenoble, France (e-mail: philippe.benech@minatec.grenoble-inp.fr).

Most location techniques are based either on the received signal strength indication (RSSI), or on the phase shift [9]. Phase variation measurement is more accurate than RSSI and less perturbed by geometric parameters (tag height, polarization angle, antenna orientation). Phase-based tag location techniques [9] are claimed to reach centimeter to millimeter accuracy, when combined with multiple frequencies [10], signal strength and accelerometric data [11], a synthetic aperture moving antenna [12], a moving tag with multiple antennas [13], and multiple tags and antennas [14].

In RFID sensing, the tag is equipped with a sensor, but the analog to numeric conversion is realized either at the tag level when it has a dedicated sensor [15], or by the interrogator when the sensed data is within the backscattered wave properties [16]. The former is more accurate, whereas the later keeps simpler electronic circuits and consumes less energy. In this last case, the tag antenna itself acts as a sensor, and modifies the properties of the backscatter link. This modification is measured by the reader through signal strength, tuning frequency or phase. Phase-based sensing is recent and has the advantage of not necessarily deteriorating the signal strength, which improves the tag reliability, reading distance, and resolution. It has been used for sensing crack opening [17] and air humidity [18].

Phase-based experiments from existing literature were conducted indoors or lasted less than one hour. In such conditions, the phase offset φ_0 is assumed constant and removed from measurements through calibration. However, during long, outdoor experiments (days, weeks or months), meteorological variations may cause significant phase offset drifts. Such drifts should be removed for location and sensing applications.

Literature on outdoor tag location includes locating objects on a construction field [19]–[23], locating tags in rivers [24]–[26], glaciers [27], and landslides [28], testing a location method on a roof [29], and tracking motions of a person [30], a train [31], or an unmanned aerial vehicle [32].

Existing literature shows environmental variations as either parameters that are measured, sources of energy loss, or sources of device deterioration. From this study's point of view, they are all considered as sources of drift. Such variations include temperature [33]–[41], air humidity [37], [42]–[45], moisture [46]–[52], snow [53],

light [54], object proximity [55]–[58], and mechanical strain [41], [58], [59]. Over long observation times, [60] shows a signal strength drift in static laboratory conditions over eight hours, and [61] studies tags durability outdoors over a six-year period. However, those studies are based on energy levels and do not study the phase.

The effect of meteorological conditions on environmental phase drift has rarely been addressed for two reasons. Firstly, radio-identification location has been developed by electronic and radio laboratories for indoor tag location tracking. Secondly, global navigation satellite systems (GNSS) already provide a robust outdoor localization. However, the recent developments in RFID techniques now allow for phase measurement with off-the-shelf and low-cost interrogators, which increases the accessibility of phase-based RFID applications for research, and its robustness for outdoor applications.

This paper aims to identify and correct the meteorological effects on the phase. Firstly, it quantifies the effect of the following meteorological variations over the phase shift: 1) water presence over a tag or a base antenna; 2) temperature of the cable, tag and base antenna; 3) moisture content of a tag wood support; and 4) atmospheric conditions of the air. Secondly, it proposes techniques to reduce those effects, and apply them on a new acquisition system. Finally, it tests this system outdoors for five months, to evaluate its accuracy and validate the corrections under real, natural conditions.

II. Method and Experimental Protocol

In free space, the phase shift related to the direct propagation of a two-way backscattered wave is given by

$$\varphi_{air} = -\frac{4\pi f}{v} d \tag{1}$$

where

- φ_{air} phase shift resulting from the propagation in the air;
- d distance between the base and the tag;
- v RF wave velocity in the medium;
- f carrier frequency.

In real conditions, the measured phase also includes the propagation in the instruments, as in

$$\varphi_{total} = \varphi_{base} + \varphi_{air} + \varphi_{tag} \tag{2}$$

where

- φ_{total} phase shift measured by the interrogator;
- φ_{base} phase shift resulting from the propagation in the reader, cable, and base antenna;
- φ_{tag} phase shift resulting from the tag backscattering.

Each of these terms is prone to variations.

φ_{air} is influenced by the propagation environment between the base antenna and the tag, such as the transmitting medium, reflectors, and scatterers. This term is almost independent from the RFID instruments, and its variations differ between each tag. This term is useful for localization applications.

φ_{tag} variations mostly depend on the tag electronics and on the antenna properties. The environmental conditions may influence it, from coupling/detuning effects, or impedance variation with temperature. These effects may be different for each tag. This term is useful for phase-based sensing.

φ_{base} variations depend on the reader electronics, cable properties, and base antenna. This effect is the same for all tags, and can be corrected by a reference tag. However, since φ_{tag} and φ_{air} are different for each tag, that would add uncontrolled variations.

The first challenge for outdoor applications is to account for the changes in meteorological parameters (rain, air moisture, temperature), which vary over time, and are likely to strongly influence phase measurements. Indeed, each instrument part (tag, cable, antennas) or medium (air and materials near the antennas) may react to meteorological changes, modifying the three phase terms in equation (2). Our purpose is to evaluate in a systematic way the effect of the meteorological conditions (mainly water and temperature) on the phase variations related to instruments, antenna detuning, and direct propagation. Multipathing, which is the combination of direct and indirect propagation, is not studied here. The experiments are designed to minimize its effect, by studying short-time variations and by using highly directive antennas.

In this article, the term *variation* represents a fluctuation of a measurable quantity over time, which includes a true variation of the measured quantity together with an added error. An *error* comes either from a bias or from random noise. A *bias* is an error that is systematic and repeatable over a short interval of time. A *drift* is a bias that is influenced by an uncontrolled parameter that varies over long periods of time. The *precision* is an indicator of random noise, the *accuracy* is an indicator of bias, and the *stability* is an indicator of drift. The scope of this article is focused on methods for improving phase stability. The precision and accuracy are not studied because results are averaged and present only relative phase variations, respectively.

The next section presents several experiments to quantify the effect of each meteorological factor on the phase. The experiments were performed outside and in a rural area, (see Fig. 1.a,b), to exclude indoor multipathing and reduce human interactions. Each experiment consisted in varying one meteorological parameter (temperature, water) and studying its effect on one element of the measurement system (cable, tag, tag support, base antenna). The experimental durations were short enough to limit the effect of other meteorological drifts, and a control measure was used to verify that there was no drift from uncontrolled parameters.

The material used in the experiments is presented in Fig. 1.c,d. Each tag (Confidex Survivor B) consisted of a quarter-wavelength patch antenna, separated by a foam insulator, protected by a hard-plastic casing, and based on a battery assisted chip (EM 4325 from EM Microelectronic). This chip has an internal temperature sensor, with 0.25 °C resolution and 1 °C accuracy. We chose a commercial, off-the-shelf, monostatic interrogator with four channels (Impinj SR420), controlled by a custom software based on the manufacturer toolkit (Octane SDK Java). Each tag interrogation acquired the phase shift, the reader internal temperature, the interrogator's time, and the temperature of the tag. We performed preliminary tests, showing that the phase was not sensitive to the interrogator temperature between -10 °C and 50 ° C.

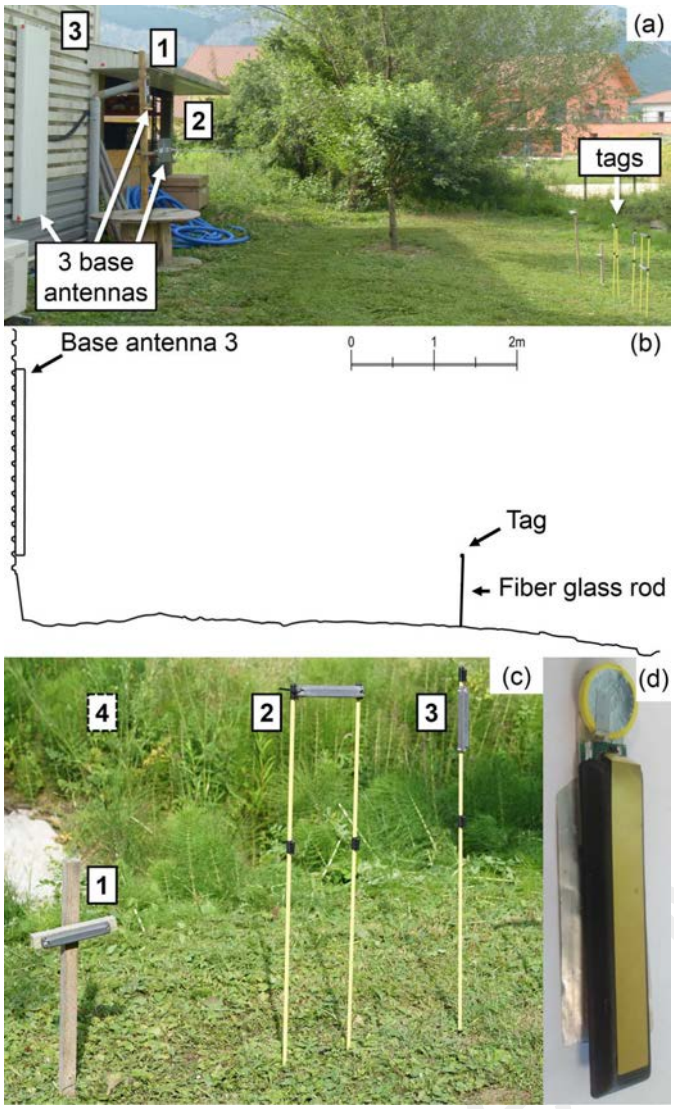

Fig. 1. System deployed outdoors, with (a) initial, intermediate and new system side by side, represented respectively with antenna 1,2 and 3, (b) two-dimensional profile of the new system obtained by terrestrial laser scanning, (c) tags on their support, with tag 1 from the initial system and tags 2-3 (4 was added later) from the new system, and (d) a tag under its casing.

This article used data from three different systems that we will name the *initial*, *intermediate*, and *new system*. The initial system was composed of a horizontally polarized slot antenna (Impinj Threshold, 5 dBi), an 8-m-long coaxial cable (type RG-58-C/U) with solid, polyethylene insulator and a 40-cm-high wood stake to support the tag. The intermediate system was composed of a Yagi-Uda antenna (14 dBi, 1-m-long), a 15-m-long coaxial cable (type RF 240) with polyethylene foam insulator and the same wood supports. It was mostly used because of its higher read range outside. The new system was composed of a 5-m-long phase-stable cable (PhaseTrack LS240, from Time Domain), a radome-protected panel antenna (Kathrein 80010643, 21 dBi, X-Pol, 3-dB radiation angle of 8° vertical and 35° horizontal), non-porous tag support (0.9-m-high fiber-glass stakes, planted 0.25m below the ground), and super-hydrophobic coating on the tag (Neverwet). This system was designed to reduce the phase drift from meteorological factors, and was tested in outdoor conditions for five months. The use of the highly-directive 21 dBi base antenna, combined with tags placed at a short distance, contribute to reduce the impact of the ground-reflected path: its orientation is 28° downwards (Fig. 1.b), which is out of the main lobe of the antenna radiation pattern.

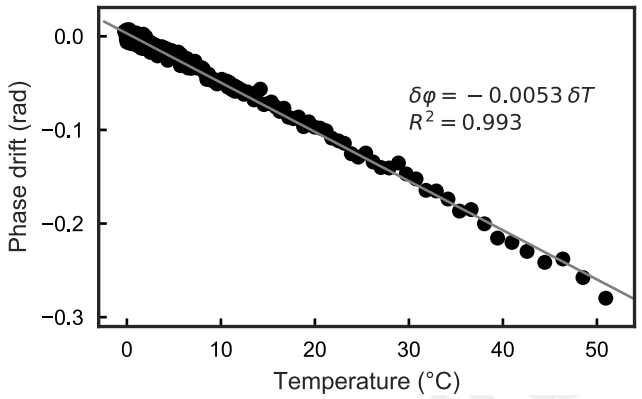

Fig. 2. Phase drift versus temperature, during the cooling down of a tag, with a linear slope of -5.3 mrad/°C.

The interrogator was configured on 30 dBm output power, 865-868-MHz carrier frequencies [62], [63], with approximately 20 asynchronous readings per second. During the processing, the phase was wrapped within $[0, \pi]$, and initialized at zero to quantify the drift. A meteorological station (Davis Vantage Pro 2) measured relative humidity, rainfall, pressure, and air temperature.

The instrument position was measured at different dates over four months using a scanning Lidar (Riegl VZ 400), to monitor instrument motions, with an error estimated at 6 mm. The motion of the instruments had also been measured with an infrared laser theodolite (Leica TCR805), placed 14m behind the tags for two hours with a precision measured at 1 mm.

Each experiment was repeated two to five times, using the same device, with slight modifications of the experimental protocol, and showed reproducible results.

III. Experimental Results

A. Effect of the Tag Temperature

To evaluate the effect of the tag temperature on the phase, a hydrophobic tag was first immersed in water, at 60°C for 20 minutes, to stabilize the tag temperature. We used water for its high calorific capacity and temperature stability. Then, we rapidly removed the tag from the water, dried it and placed it on a wooden, outdoor support. The tag remained motionless. Its temperature decreased and stabilized around 0°C after 35 minutes. The meteorological conditions were dry, with no sun and 0°C air temperature. Fig. 2 shows the phase, depending on the temperature measured by the tag. The phase shows a linear relationship with the temperature, with a negative slope of 5.3×10^{-3} rad/°C.

To estimate a yearly phase drift, we evaluate a yearly tag temperature range from 0°C to 60 °C, affected by air temperature and radiative heating. Such a temperature variation

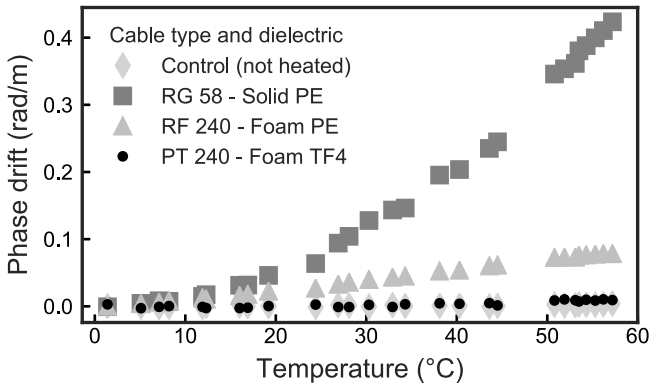

Fig. 3. Phase drift versus temperature, normalized to 1-m-cable-length, for three different types of coaxial cables, and one control cable that was not heated.

corresponds to a possible phase error of 0.37 rad, which represents a relative ranging error of 10 mm.

This instrumental and detuning effect is not characterized by constructors of tags and micro-circuits, and may differ between tag constructions. It may originate from the tag's antenna [64], printed circuit board [65] or integrated circuit. It could be cancelled by a specific tag conception, or by calibrating the effect and measuring the tag temperature.

B. Effect of the RF Cable Temperature

The effect of temperature on the characteristics of coaxial transmission cable has been previously studied [66]–[68]. It was first shown that temperature has an impact upon the cable electrical length, resulting from thermal expansion of the cable assembly, and change in dielectric permittivity of the insulator material, such as polyethylene or Teflon-PTFE [69].

To evaluate the effect of temperature on different cables, we plunged a large portion of each cable into a recipient of tap water. The water was initially mixed with ice, to remain at a temperature of 0°C, and then heated step by step by adding boiling water. The temperature was measured at each heating step and during its natural decrease, and is associated to a phase averaged over 10s.

Fig. 3 shows the bivariate representation of the phase and temperature, at each temperature measurement. The RG58 cable shows a quadratic relation with temperature, and the RF240 and PT240 show linear relationship, which are summarized in Table I.

The relative wave velocity is 66% in the RG58 (from the relative permittivity $\varepsilon_r = 2.3$ of solid polyethylene [70]), and 83% in the RF240 and PT240 (from specifications). To compare the results independently from frequency, the relative electrical length variation is calculated by using (1) after correcting the total electrical length with the relative wave velocity. The relative electrical length variation reported in Table I, for the PT240 cable, is coherent with the specifications. However, for the solid-polyethylene-based cable, the literature reports a value that is twice smaller than the one we measured, at 400 MHz for the 25-55°C temperature range [67]. The different cable assembly may explain the difference.

TABLE I
COMPARISON OF THE PHASE VARIATIONS FROM TEMPERATURE, FOR DIFFERENT COAXIAL CABLES

Cable	Phase variation (mrad/m)	Electrical length variation (ppm/°C)	Variation, from literature / specs (ppm/°C)
RG58	0.13 x T^2	181 (25-55°C)	87 (25-55°C)
RF240	1.5 x T	34	-
PT240	0.21 x T	5.3	5 (0-60°C)

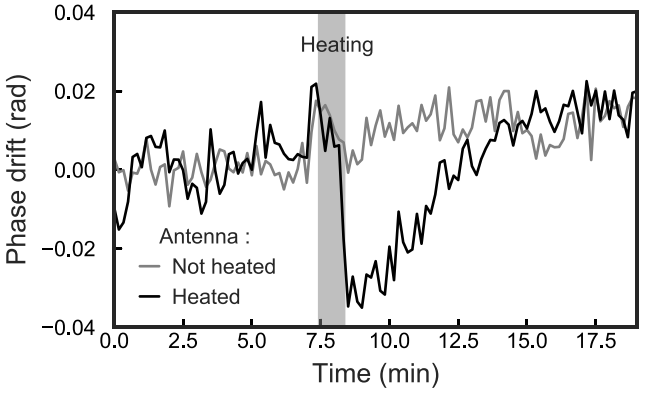

Fig. 4. Phase drift versus time when heating an aluminium Yagi antenna. The variation with an unheated antenna is shown for comparison. The y-axis scale is smaller than on other figures.

A typical yearly temperature variation of 0-60°C, over an 8-m-long cable, would induce a phase drift between 4.7 radians and 0.13 radians, respectively with RG58 and PT240 coaxial cable.

This is an instrumental effect, characterized by constructors of phase-stable cables, and independent from the tag. It could be reduced by choosing an appropriate cable assembly, by keeping the cable as short as possible, by estimating the cable temperature, or by limiting the temperature variation, either passively, for example by burying the cable, or with a temperature control.

C. Effect of the Base Antenna Temperature

To evaluate the effect of the antenna temperature on the phase, a fixed Yagi-Uda antenna was heated with a heat gun (P = 2 kW) for one minute, with regular movements over the whole antenna, holding the gun at an approximate distance of 10 cm. The antenna temperature started at 12 °C, and reached approximately 50 °C, evaluated from the same procedure applied on an independent temperature sensor. A control antenna remained 30 cm away from the heat gun. After heating the antenna, the operator went away.

Fig. 4 shows the phase measured through the two antennas over time. A negative phase drift of 0.03 rad is observed while heating the antenna (t = 7.5-8.5 min). The phase drift progressively goes back to null after 7 minutes, while the antenna cools down. In a linear approximation, this variation represents -8×10^{-4} rad/°C.

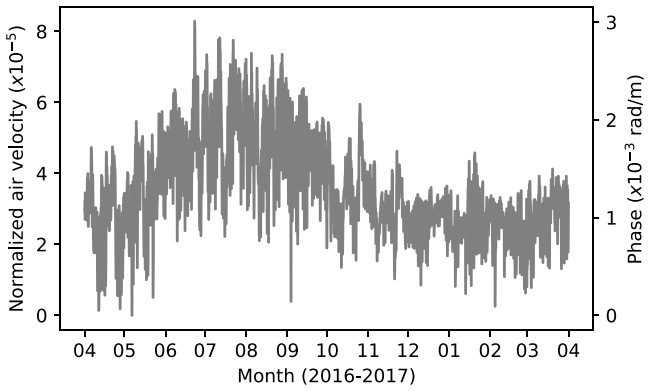

Fig. 5. Model of the relative variation of air velocity, and phase variation per distance between the antenna and tag, for a year, based on meteorological data.

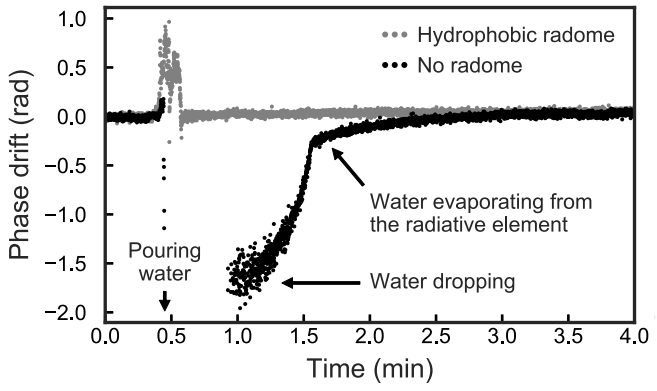

Fig. 6. Phase drift versus time when pouring water on a base antenna that is unprotected, or that is protected with a hydrophobic radome.

A temperature antenna of 0-60°C would create a phase error of 0.05 radians, or 1.3 mm relative ranging error, which we consider negligible for our application.

This instrumental effect is not characterized by constructors, and it is independent from the tag. It may vary significantly depending on the antenna, especially if it contains temperature-sensitive dielectric materials. It could be corrected by calibrating and measuring the temperature antenna.

D. Atmospheric Conditions on Wave Velocity

Wave velocity in the low troposphere at ultra-high frequency depends on atmospheric conditions [71], with a celerity ratio n given by:

$$n - 1 = 77.6 \times 10^{-6} \frac{P}{T} + 3.73 \times 10^{-1} \frac{e}{T^2} \quad (3)$$

where

P atmospheric pressure (hPa);
e water vapor partial pressure (hPa);
T absolute temperature (K);

As this value depends on several parameters, we will estimate its real drift over a year, with real meteorological data, obtained from a local station (Le Versoud, France). The partial vapor pressure e is derived from the saturated vapor pressure calculation in [72], using

$$e = RH \times 6.1078 \exp\left[\frac{17.2693882(T - 273.16)}{T - 35.86}\right] \quad (4)$$

where RH is the relative humidity (no unit), provided from the meteorological station.

The resulting variation in air velocity is shown in Fig. 5. The velocity variation is converted as a phase drift, normalized for one-meter distance between the tag and antenna.

A typical application with 10 m free air range between the tag and base antenna, would imply a yearly phase drift of 0.03 rad, or 0.8 mm relative ranging. This effect is negligible at such a distance, but should be taken into account for larger distances.

This effect concerns direct and indirect propagation. It is generalizable for air transmission, but not other mediums such as water, vegetation or snow. As soon as the air is the only propagation medium, this effect can be corrected, by measuring the atmospheric condition with a meteorological sensor, and estimating the absolute tag range.

E. Effect of Water Over the Base Antenna

The presence of droplets or a thin layer of water on antennas, resulting from rain or condensation, is a well-known problem in radar [73], as it attenuates the signal but also modifies its phase. To reduce this effect, radomes are commonly used in combination with various types of hydrophobic surfaces [74].

To simulate the effect of rain or condensation, an operator poured a jar of 1000 ml of tap water everywhere over two motionless Yagi-Uda base antennas, in 10 seconds. The first antenna was unprotected, whereas the radiating element of the second antenna was protected with a radome coated with a super-hydrophobic layer [75] (Neverwet). This outdoor experiment lasted four minutes, fast enough to consider other meteorological parameters as constants. The air relative humidity was 46%, and the temperature was 29°C (air) and 35°C (tags).

The phase-time curves are shown in Fig. 6, for the antennas with and without protection. Water is poured on the unprotected antenna at t = 0.45 min, and shortly after on the protected antenna. For the antenna protected with a hydrophobic radome, a short positive phase drift of about 1 radian is observed, which results from the presence of the operator. After 0.7 min, the curve is perfectly flat. In contrast, with the unprotected antenna, there is a total communication loss from 0.45 min to 0.8 min, followed by a strong negative phase drift peak of about 2 rad, which decreases rapidly until reaching 0.3 rad at t = 1.6 min. Then, the phase regularly increases, and returns to a null value after 2.5 min. The fast decrease corresponds to water that drips and form droplets, whereas the slow decrease corresponds to water evaporation, which was rapid due to elevated temperature and low humidity.

Using (1) these effects corresponds to a temporary ranging error of 55 mm for the maximum peak, and 8 mm for the slower decrease. This detuning and tag-independent effect is

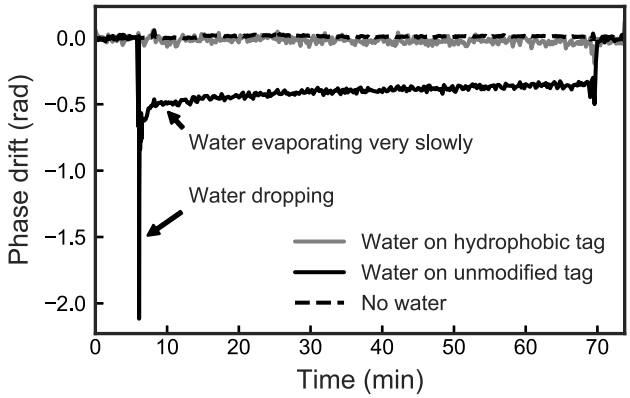

Fig. 7. Phase drift versus time when pouring water on a hydrophobic and non-hydrophobic encapsulated tag. The phase variation for a dry tag is shown for comparison.

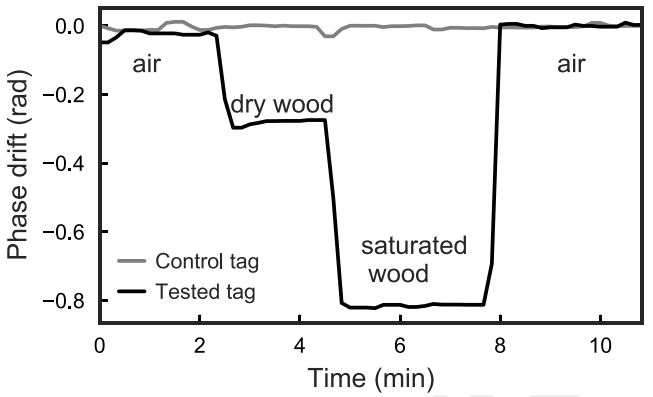

Fig. 8. Phase shift versus time with different moisture contents of the support material placed behind the tag: free air, and wood with 0% and 44% water content.

not characterized by traditional constructors. This experiment highlights the efficiency of an hydrophobic radome to protect the antenna from water and cancel its effect.

F. Effect of Water Over Tags

To simulate the effect of rain or condensation on tags placed outside, an operator dropped 25 ml of distilled water at ambient temperature (T = 7±1 °C, no sun), on two hard-cased tags, either unmodified, or coated with a super-hydrophobic layer (Neverwet). Later (t = 70 min), the operator gently dried the tag with a disposable tissue. The tags were attached on a hydrophobic plastic stick to avoid water on the support. A third tag remained dry for control. The operation of dropping water lasted 10 sec. The relative humidity was measured at 74±2 % during the whole experiment.

Phase measurements on Fig. 7 reveals that water induced firstly a negative phase peak of 2.1 radian on the standard tag (equivalent to 58-mm ranging error), followed by a slow decrease starting from 0.5 rad (14 mm) while the water slowly evaporated. The return to zero was obtained after the operator dried the tag. Visual control showed that water formed a thin layer over the surface just after pouring water, which rapidly aggregated into droplets, that almost did not dry (compared to Fig. 6) because of cold and humid conditions. The phases of the control tag and hydrophobic tag remained stable.

This detuning and tag-dependent effect is not characterized by tag constructors. An external water protection could cancel the effect independently of the tag type. This experiment again shows the efficiency of the super-hydrophobic coating that removes the effect of water on the tag, as in [76].

G. Moisture of the Material Supporting the Tag

In outdoor conditions RFID tags have to be attached on a stake, made of non-metallic material, to avoid affecting antenna performance [57] or increase multipathing complexity. Many RFID experiments use wood stakes that are inexpensive and easy to shape. However, wood is porous and contains moisture. Moisture varies with rain, air humidity and temperature, and may be inhomogeneous over the wood volume. The moisture content is defined as the ratio between the mass of water and dry wood. It typically varies between 10 to 25% within a year outdoors [77], and by 2% per day on the first centimeter of the material, when exposed to high air humidity [78]. The moisture content modifies the dielectric properties of wood [79] and thus shifts the phase. This effect is exploited in [80], to track the moisture content of a cork wine-bottle-cap with a tag.

The following experiment investigates the effect of the moisture content on the phase. A piece of pine-wood (dimension 35x35x125 mm, density = 0.40) was oven dried at 105 °C for one hour, and a second identical piece was saturated with water in a vacuum chamber. Their moisture content was respectively 0.3 % and 44 %, measured by weight difference after drying the pieces in a 105-°C oven for 24h. On step one, a tag was fixed on a plastic support, designed to leave free space behind the tag. On step two, we placed the dried wood behind the tag, in contact with its plastic casing, without moving the tag. On step three, we removed the dried wood and placed the saturated wood instead. On the last step, we removed the wood, to return to the initial conditions.

Fig. 8 shows the phase shift, while changing the tag background sequentially with air (t = 0), dry wood (t = 2 min), saturated wood (t = 4.3 min), and air again (t = 8 min). The presence of dry wood behind the tag shifts the phase by 0.3 rad, and the 44% moisture content shifts the phase by another 0.5 rad. In a linear approximation, that corresponds to a variation of 12 mrad per percent of moisture content. After removing the background material, the phase returns to its initial state.

It is difficult to estimate a typical variation of moisture content over a year: this parameter has different dynamics depending on the depth considered, and varies from one material to another. As an estimate of a maximal yearly drift, we will use the phase difference between dry and saturated wood in our experiment, which is 0.5 rad. That is equivalent to 14 mm in relative ranging.

This detuning effect is similar to the effect of water on the tag. It could be eliminated by changing the tag support, whatever the tag. To correct this effect, one may use non-porous support, or separate the tag from its support with a metallic reflector.

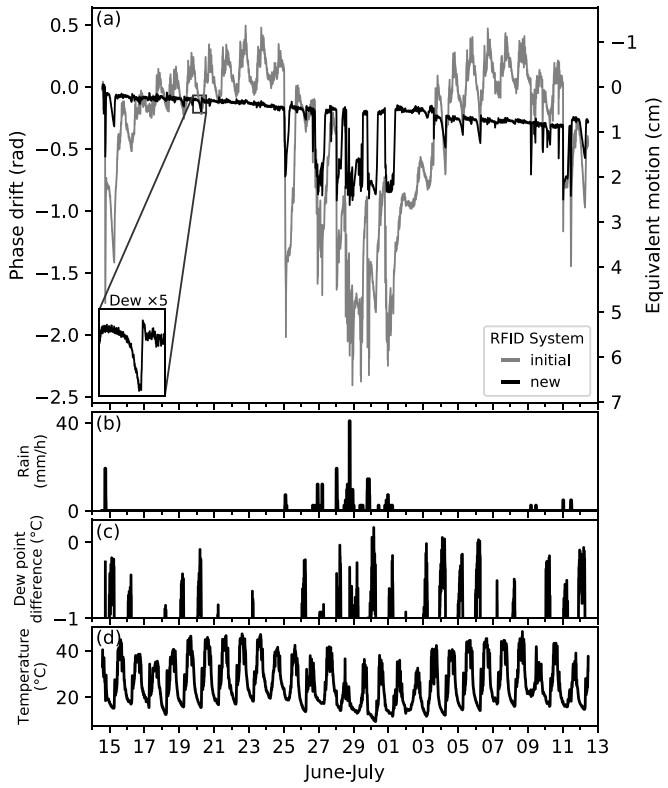

Fig. 9. Variation over one month of (a) the phase for different RFID systems, for initial (tag 1, antenna 1) and new system (tag 2, antenna 3), along with (b) the measured rain rate, (c) the difference between tag temperature and dew point, that suggest the condensation of a water film when above a certain point, and (d) the temperature measured by the tag sensor.

IV. Validation

A. Overview of the New System

To validate the experimental results and the efficiency of the corrections, a static installation was set outside, for one month. It compares the evolution of the phase, between an initial system, and a new system that corrects for phase drift.

The initial system is composed of a standard slot antenna, a coaxial cable provided by the interrogator manufacturer, and a hard-cased tag attached on a wood support. In comparison, the new system is numerically corrected for tag temperature (from a temperature sensor on the tag), and physically corrected for cable temperature (with temperature-stable cables), moisture of the tag support (with fiber glass stakes), water on the tag (with super-hydrophobic coating), and water on the base antenna (with radome-protected antenna).

Fig. 9.a presents the phase drift over one month, and Fig. 9.b-d presents rain, dew indicator and tag temperature, obtained from a meteorological station on site, and from a temperature sensor within the tag. The phase varies from 0.50 to -2.50 radians (3.0 rad total) on the initial system, and from 0 to -0.95 radians on the new system. The accuracy of the new system has improved by a factor of 3 over the whole period. However, this accuracy may depend on the period considered. It is separated in the next sections into water-related drift, temperature-related drift, and residual unidentified slow drift.

B. Water Effect

Rain forms a water layer on the tags and base antenna, which impacts the phase. The rain on Fig. 9.b shows a strong and systematic impact over the phase. For example, during heavy rain on June 28th, the phase decreases of up to 2.3 radians on the initial system, and up to 0.7 radians on the new system. Besides, heavy rain creates a negative phase offset on the initial system, which takes a day or more to decrease, as observed after the rain episodes of June 14th and 29th. This offset comes from the moisture of the wood tag support, that is slow to dry, and influence the phase, as shown in Fig. 8.

Dew forms a water layer on the tags and base antenna, when radiative heat loss decreases their temperature below the dew point. It happens mostly outdoors at night, from radiative heat loss. Fig. 9.c shows the difference between the tag temperature and the dew point, provided by the meteorological station. A positive difference (within the 1°C accuracy of the tag sensor) indicates dew formation on the tags, and on objects with the same temperature. This indicator clearly correlates with negative phase peaks on Fig. 9.c, which often appears between 24h-6h. The dew effect varies from almost no variation (e.g., on June 20th at 6:00), to 0.7/0.25 rad on the former/new system respectively (on June 15th, just after a rain episode).

The effect of water was reduced by a factor of 3, both for rain and dew formation, between the initial and new system. This residual effect results from the observed water accumulation on the tag and antenna, even with the new system. Also, it was observed (not presented) that the water effect amplitude on the vertically-polarized tags 3 and 4 was reduced by a factor of 2, simply because the vertical shape accumulates less water on top of the tag. A specific design of the tag and its casing may better correct this effect, which is out of this study scope.

C. Temperature Effect

Fig. 9.d. shows the temperature measured by the tag, which differs from air temperature by radiative heat transfers. The temperature shows a positive correlation with the phase of the initial system, and no visible correlation on the new system, which is a good improvement.

The phase-temperature ratio was previously measured at -5 mrad/°C for the tag (Fig. 2) and 0.13 mrad/°C^2/m for the solid polyethylene cable (Fig. 3). Within a 15-45°C temperature interval, the expected daily drift on the initial system is 1.4 radians, however, Fig. 9 shows only a drift of 0.8 radians. The cable temperature is prone to less daily variations, due to lower sun exposition, which may explain the difference.

D. Slow Drift

Apart from rain and temperature effect, the phase on the new system seems to show a slow drift, of approximately 0.3 rad over the month. To further investigate this residual slow phase drift, the phase was observed for five months, with three hydrophobic tags attached on non-porous stakes (tags 2-4 on Fig. 1.c). The tag 2 was used in the new system, presented on Fig. 9. It was attached with two fiber-glass stakes and a horizontal polarization. The tag 3 was vertically polarized and

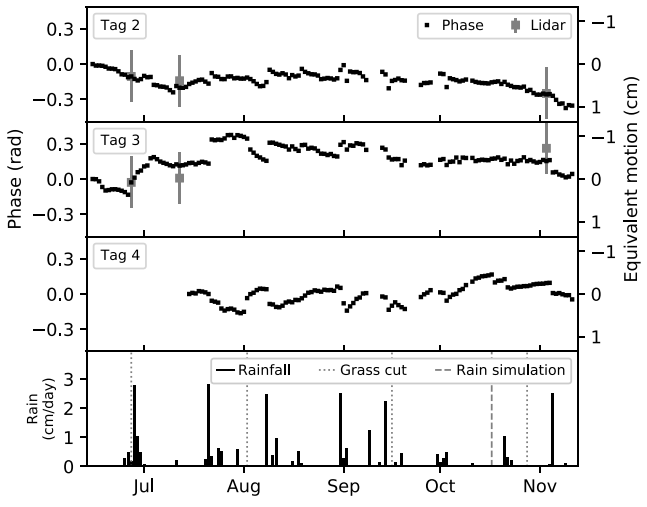

Fig. 10. Daily phase (95th percentile), and motion estimated by LiDAR scanning, for three different tags, over five months, along with the daily rainfall. The four dotted vertical lines represent the intervention of a gardener to mow the grass, and the dashed vertical line on October 17th represents a rain simulation.

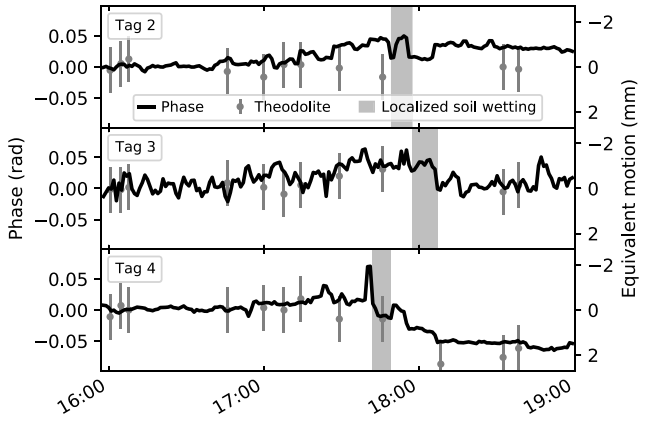

Fig. 11. Phase along time, for all the tags tested, when simulating a rainfall event, along with relative motion measured by an independent theodolite. The grayed zones represent pouring higher quantity of water at the base of the stakes that support the tags.

attached on one single stake, to see if the tag polarization had any effect on the phase drift. Finally, the tag 4 was sealed in a 70-cm-deep and 10-cm-large hole, filled with concrete, and vertically polarized. It replaced tag 1 on July 14th, to reduce a potential motion of the stakes.

Fig. 10 shows the slow drift of those three tags, by showing the daily 95th percentile. A previous test showed no meaningful change on the result between the 90th and 98th percentile, which proves the method robust on this dataset, to remove the residual effect of rain and dew, and focus on slow drift.

1) 5-Month Trend: The phase drifted by an average amplitude of 0.05-0.11 rad (1.4-2.8 mm) per month over five months, depending on the tag considered. The phase of tag 2 slowly decreased by 0.28 rad the first month, plateaued the following three months and decreased by 0.22 rad during the last month. The phase of tag 3 increased steeply by 0.5 rad the first month, decreased by 0.09 rad/month until September 27th and finished by a plateau. The phase of tag 4 showed no clear trend. It is globally hard to see any relation between the very slow drift of each tag.

2) No Multipathing Influence From Vegetation: The dotted lines on Fig. 10 show the intervention of a gardener, who mowed the grass. Those interventions did not have significant effects on the phase, either on the long-term or by zooming on the event (not presented here), except on August 2nd when the tags 3 and 4 moved during the operation. A special care was taken on July 27th, where the grass was weighted (1.3 kg/m2 wet, 0.20 kg/m2 dried, height below 30 cm) and measured by Lidar, and the gardener operation carefully reviewed, but the phase did not change. It changed only a few hours later, with the rain.

3) Motion of the Tags Detected by Lidar Measurement: A scanning Lidar acquired the geometry of the environment in 3 dimensions, on June 27th, July 12th, and November 3rd, that allowed for comparison across time. The comparison showed no significant translation or tilt of the base antenna, compared to immobile reference targets. There was, however, a motion of the tag, quantified from a tilt of the stake, and a variation of distance with the base antenna. This motion influences the phase, and as a consequence, the slow variation is explained partly by a residual undesirable drift and partly by a true motion.

4) Influence of the Rain: The slow variation of the phase was clearly impacted by rain, especially observed during important episodes. The most impactful event, on July 21th, changed the phase by +0.09, +0.2 and -0.06 rad, respectively on the tags 2,3, and 4. On tag 2, the rain had no consistent effect on the phase. On tag 4, the rain consistently decreased the phase. On tag 3, the rain increased the phase until July 21st and decreased it after this date. To conclude, the rain had an effect on the phase, but it was not consistent over time and between tags. A part of this variation could have been caused by a tag motion: a changes of rigidity, shape or pressure of the soil, may result from water content variations [81] or variations in the roots network, and induce a tilt of the tag stakes.

The next section presents an experiment to test if the rain can move the tags, which would explain this influence on the phase.

E. Motion Induced by Simulated Rain

To better understand the rain-related slow-drift, we simulated the effect of rain on the soil. On October 17th (showed by a dashed line on Fig. 10), we poured 50 L of water (conductivity 32 mS/m, temperature 19.1 °C), equivalent to 5 cm of rain over 1m^2, at the base of the stakes that support the tags, without wetting the tag. The tag position was measured regularly with a laser theodolite. Prior tests showed that wetting the environment and the potential reflectors (vegetation, ground) had no significant effect on the phase, which again confirmed that indirect path were negligible in this experimental design.

Fig. 11 shows that dropping high quantities of water near the stakes had a clear effect on tag 4, a slight effect on

tag 3, and no significant effect on tag 2. The phase of tag 4 progressively dropped by 0.06 rad (2 mm), from 17h40 to 18h05, right after pouring the water on the tag stake. A similar 2-mm-decrease was observed independently with the theodolite, which confirms the displacement. This phase variation is also visible as a jump on Fig. 10, which effect remained for several days. Furthermore, the following important rain events, on October 21st and November 5th, also decreased the phase by a similar magnitude, which suggests that the motion of the tag 4 was a major cause of rain-related phase drift. From this experiment it can be concluded that water can move the stakes that support the tags, even with a 70-cm-deep concrete sealing, and that this effect has the same magnitude as the slow drift that happen during rain events.

The motion of the tag is therefore an important part of the slow drift. There remains an unidentified contribution, which can be estimated at a maximum of 6 mm over the 4-month interval of Lidar measurement, deduced from the Lidar precision. This corresponds to a maximal drift (not related to motion) of 0.05 rad/month, of 1.5 mm/month.

V. Conclusion

We identified significant meteorological effects on the phase measurements, the magnitude of which is given in Table II. For a typical installation with an 8-m-long polyethylene cable, 10-m range between tag and base antenna, and 60 °C of object temperature variation under the sun, the factors of greatest influence are the water layer over the base antennas and tag (4.1 rad) and the cable temperature (3.7 rad). Factors with smaller influence are the tag temperature (0.3 rad) and the material moisture (0.5 rad). The temperature of Yagi antenna temperature (0.05 rad), and the meteorological variations of the air (0.03 rad) have a negligible influence. Some effects are opposed, such as the temperature of the tag and of the cable, and might be partially cancelled. Combining the different effects shown in table II may lead to an error of up to 8.1 rad within one year of operations, where the drift reaches its minima for high humidity and low temperature, and maxima for the opposite. In terms of positioning, one may expect a drift of about 22 cm in relative ranging over a year from meteorological effects, which is to be compared with the centimeter accuracy reported in the literature for absolute ranging indoors during short times. In terms of sensing, this is far beyond the sensor dynamic reported in [16] and [17], which is typically from 1 to 2 rad.

Specific solutions have been proposed for each identified effect to reduce the phase drift. A hydrophobic and hermetic radome avoids the creation of a water film from rainfall and condensation. The cable temperature effect is reduced by using shorter cable with phase-stable assembly and insulator. The tag temperature effect is corrected by using an integrated circuit that includes a temperature sensor. The problem of moisture content is reduced by attaching the tag to a non-permeable material such as plastic or fiber glass. The variation of wave velocity in the air is corrected by measuring the air temperature, pressure and relative humidity over the area. Finally, the antenna temperature is corrected by installing a temperature sensor near or within the antenna. These corrections are independent of the tag construction, except for the water protection, the efficiency of which depends on the tag design, and for the temperature correction which requires the calibration of each tag.

TABLE II
Sources of Phase Drift in Outdoor Conditions

Effect	Variations (mrad)	Yearly drift (rad)	Yearly drift (mm)	Solution
Water on base antenna.	-2000	2.0	55	Hydrophobic radome.
Water on tag.	-2100	2.1	58	Hydrophobic radome.
Cable temperature (Polyethylene).	0.13 /°C²/m	3.7	102	Phase-stable short cable.
Tag temperature.	-5 /°C	0.3	10	Temperature sensor.
Wood stake moisture.	-12 / %	0.5	14	Impermeable material.
Antenna temperature (Yagi)	-0.8 /°C	0.05	1.3	Temperature sensor.
Air refractive index.	3 /m	0.03	0.8	Meteorological data.
Total meteorological effects, expected.	-	8.1	223	

TABLE III
Comparison of the Phase Variations With the Initial and Newly Developed Systems During the 1-Month Experiment

Period considered	Initial phase variation (rad)	New phase variation (rad)	Gain in accuracy
Whole period.	3.0	0.95	3
A dry day.	0.6	0.05	12
Rain event.	2.3	0.7	3
Dew event.	0.7	0.25	3

All these solutions were implemented in a new acquisition system, which was compared for 1 month outdoors to the initial system. The new system improved the phase stability by a factor of at least 3 for the whole period, as shown in table III. It made negligible the influence of temperature, and reduced the influence of water by a factor of 3. The stability over one dry day was improved by a factor of 12, to reach 0.05 rad.

There remained slow variations over long periods, partly related to a motion of the tags, and partly related to a residual unidentified drift. This residual drit was estimated at a maximum of 0.20 rad (6 mm), compared to four-month-interval Lidar acquisitions, which corresponds to an average of 0.05 rad per month, or 1.5 mm per month.

The measured slow drift now fits with our application requirements to monitor movements between 10 centimeters and a few meters per year. Since a significant part of the phase variation came from parasitic ground-related tag motion, which may be expected to be even stronger on a landslide application, it is not worth further stabilizing the phase for slow motion monitoring.

Future works may require to better understand the impact of the multipathing on the phase outdoors, which is prone to complex and slow variations (shape and liquid water content of the soil, vegetation, and snow), and to mitigate this effect.

Other instrumental challenges may also be studied, especially under extreme temperature or humidity. A real outdoor experiment on a landslide site will be implemented to address these questions.

ACKNOWLEDGMENT

Authors thank Q. Barbier for the Lidar acquisition and processing, and H. Taylor for proofreading the manuscript.

REFERENCES

[1] J. Heidrich *et al.*, "The roots, rules, and rise of RFID," *IEEE Microw. Mag.*, vol. 11, no. 3, pp. 78–86, May 2010.

[2] R. Miesen *et al.*, "Where is the tag?" *IEEE Microw. Mag.*, vol. 12, no. 7, pp. S49–S63, Dec. 2011.

[3] G. Marrocco, "Pervasive electromagnetics: Sensing paradigms by passive RFID technology," *IEEE Wireless Commun.*, vol. 17, no. 6, pp. 10–17, Dec. 2010.

[4] J. A. Gili, J. Corominas, and J. Rius, "Using global positioning system techniques in landslide monitoring," *Eng. Geol.*, vol. 55, no. 3, pp. 167–192, Feb. 2000.

[5] A. Abellán, M. Jaboyedoff, T. Oppikofer, and J. M. Vilaplana, "Detection of millimetric deformation using a terrestrial laser scanner: Experiment and application to a rockfall event," *Nat. Hazards Earth Syst. Sci.*, vol. 9, no. 2, pp. 365–372, Mar. 2009.

[6] J. Travelletti *et al.*, "Correlation of multi-temporal ground-based optical images for landslide monitoring: Application, potential and limitations," *ISPRS J. Photogram. Remote Sens.*, vol. 70, pp. 39–55, Jun. 2012.

[7] G. Herrera *et al.*, "A landslide forecasting model using ground based SAR data: The Portalet case study," *Eng. Geol.*, vol. 105, nos. 3–4, pp. 220–230, May 2009.

[8] J. D. Kenney *et al.*, "Precise positioning with wireless sensor nodes: Monitoring natural hazards in all terrains," in *Proc. IEEE Int. Conf. Syst. Man Cybern.*, San Antonio, TX, USA, 2009, pp. 722–727.

[9] P. V. Nikitin *et al.*, "Phase based spatial identification of UHF RFID tags," in *Proc. IEEE Int. Conf. RFID*, Orlando, FL, USA, 2010, pp. 102–109.

[10] C. Zhou and J. D. Griffin, "Accurate phase-based ranging measurements for backscatter RFID tags," *IEEE Antennas Wireless Propag. Lett.*, vol. 11, pp. 152–155, Jan. 2012.

[11] M. B. Akbar, D. G. Taylor, and G. D. Durgin, "Hybrid inertial microwave reflectometry for mm-scale tracking in RFID systems," *IEEE Trans. Wireless Commun.*, vol. 14, no. 12, pp. 6805–6814, Dec. 2015.

[12] R. Miesen, F. Kirsch, and M. Vossiek, "UHF RFID localization based on synthetic apertures," *IEEE Trans. Autom. Sci. Eng.*, vol. 10, no. 3, pp. 807–815, Jul. 2013.

[13] Z. Wang, N. Ye, R. Malekian, F. Xiao, and R. Wang, "TrackT: Accurate tracking of RFID tags with mm-level accuracy using first-order Taylor series approximation," *Ad Hoc Netw.*, vol. 53, pp. 132–144, Dec. 2016.

[14] M. Scherhäufl, M. Pichler, and A. Stelzer, "UHF RFID localization based on phase evaluation of passive tag arrays," *IEEE Trans. Instrum. Meas.*, vol. 64, no. 4, pp. 913–922, Apr. 2015.

[15] R. Want, "Enabling ubiquitous sensing with RFID," *Computer*, vol. 37, no. 4, pp. 84–86, Apr. 2004.

[16] C. Occhiuzzi, S. Caizzone, and G. Marrocco, "Passive UHF RFID antennas for sensing applications: Principles, methods, and classifications," *IEEE Antennas Propag. Mag.*, vol. 55, no. 6, pp. 14–34, Dec. 2013.

[17] S. Caizzone, E. DiGiampaolo, and G. Marrocco, "Wireless crack monitoring by stationary phase measurements from coupled RFID tags," *IEEE Trans. Antennas Propag.*, vol. 62, no. 12, pp. 6412–6419, Dec. 2014.

[18] M. C. Caccami, S. Manzari, and G. Marrocco, "Phase-oriented sensing by means of loaded UHF RFID tags," *IEEE Trans. Antennas Propag.*, vol. 63, no. 10, pp. 4512–4520, Oct. 2015.

[19] J. Song, C. T. Haas, and C. H. Caldas, "A proximity-based method for locating RFID tagged objects," *Adv. Eng. Informat.*, vol. 21, no. 4, pp. 367–376, Oct. 2007.

[20] S. N. Razavi and C. T. Haas, "Using reference RFID tags for calibrating the estimated locations of construction materials," *Autom. Construct.*, vol. 20, no. 6, pp. 677–685, Oct. 2011.

[21] E. Valero, A. Adán, and C. Cerrada, "Evolution of RFID applications in construction: A literature review," *Sensors*, vol. 15, no. 7, pp. 15988–16008, Jul. 2015.

[22] H. Li, G. Chan, J. K. W. Wong, and M. Skitmore, "Real-time locating systems applications in construction," *Autom. Construct.*, vol. 63, pp. 37–47, Mar. 2016.

[23] E. Valero and A. Adán, "Integration of RFID with other technologies in construction,' *Measurement*, vol. 94, pp. 614–620, Dec. 2016.

[24] I. M. Miller, J. A. Warrick, and C. Morgan, "Observations of coarse sediment movements on the mixed beach of the Elwha Delta, Washington," *Marine Geol.*, vol. 282, nos. 3–4, pp. 201–214, Apr. 2011.

[25] M. Chapuis, S. Dufour, M. Provansal, B. Couvert, and M. de Linares, "Coupling channel evolution monitoring and RFID tracking in a large, wandering, gravel-bed river: Insights into sediment routing on geomorphic continuity through a riffle–pool sequence," *Geomorphology*, vol. 231, pp. 258–269, Feb. 2015.

[26] A. G. Tsakiris, A. N. Papanicolaou, I. V. Moustakidis, and B. K. Abban, "Identification of the burial depth of radio frequency identification transponders in riverine applications," *J. Hydraul. Eng.*, vol. 141, no. 6, Jun. 2015, Art. no. 4015007.

[27] O. Rorato *et al.*, "An ad-hoc RFID tag for glaciers monitoring," in *Proc. IEEE APS Topical Conf. Antennas Propag. Wireless Commun.*, Palm Beach, Aruba, 2014, pp. 864–867.

[28] C. Lucianaz, G. Greco, S. Bertoldo, and M. Allegretti, "Real time outdoor localization of buried RFID tags through statistical methods," in *Proc. Int. Conf. Electromagnetics Adv. Appl.*, Turin, Italy, 2015, pp. 1152–1154.

[29] M. B. Akbar, D. G. Taylor, and G. D. Durgin, "Amplitude and phase difference estimation bounds for multisensor based tracking of RFID tags," in *Proc. IEEE Int. Conf. RFID*, San Diego, CA, USA, 2015, pp. 105–112.

[30] M. Polivka, M. Svanda, P. Hudec, and S. Zvanovec, "UHF RF identification of people in indoor and open areas," *IEEE Trans. Microw. Theory Techn.*, vol. 57, no. 5, pp. 1341–1347, May 2009.

[31] L. Yang, J. Cao, W. Zhu, and S. Tang, "Accurate and efficient object tracking based on passive RFID," *IEEE Trans. Mobile Comput.*, vol. 14, no. 11, pp. 2188–2200, Nov. 2015.

[32] G. Greco, C. Lucianaz, S. Bertoldo, and M. Allegretti, "Localization of RFID tags for environmental monitoring using UAV," in *Proc. IEEE 1st Int. Forum Res. Technol. Soc. Ind.*, Turin, Italy, 2015, pp. 480–483.

[33] A. A. Babar, S. Manzari, L. Sydanheimo, A. Z. Elsherbeni, and L. Ukkonen, "Passive UHF RFID tag for heat sensing applications," *IEEE Trans. Antennas Propag.*, vol. 60, no. 9, pp. 4056–4064, Sep. 2012.

[34] F. Yang, Q. Qiao, L. Zhang, Z. Yue, and A. Z. Elsherbeni, "High-sensitivity RFID sensing antennas: From sensing mechanism selections to antennas structure designs," in *Proc. 31st URSI Gen. Assembly Sci. Symp.*, Beijing, China, 2014, pp. 1–4.

[35] Q. Qiao, L. Zhang, F. Yang, Z. Yue, and A. Z. Elsherbeni, "UHF RFID temperature sensor tag using novel HDPE-BST composite material," in *Proc. IEEE Antennas Propag. Soc. Int. Symp.*, Orlando, FL, USA, 2013, pp. 2313–2314.

[36] L. Zhenzhong *et al.*, "Effects of temperature and Humidity on UHF RFID performance," in *Proc. CANSMART Workshop Smart Mater. Struct.*, Montreal, QC, Canada, 2011, p. 10.

[37] S. L. Merilampi, J. Virkki, L. Ukkonen, and L. Sydänheimo, "Testing the effects of temperature and humidity on printed passive UHF RFID tags on paper substrate," *Int. J. Electron.*, vol. 101, no. 5, pp. 711–730, May 2014.

[38] X. Yu *et al.*, "A novel temperature control system of measuring the dynamic UHF RFID reading performance," in *Proc. 6th Int. Conf. Instrum. Meas. Comput. Commun. Control*, Harbin, China, 2016, pp. 322–326.

[39] M. Mazur, W. Marynowski, A. Kusiek, and W. Zieniutycz, "Effect of time varying measurement conditions on antenna pattern in near field measurement and its correction procedure," in *Proc. 20th Int. Conf. Microw. Radar Wireless Commun.*, Gdańsk, Poland, 2014, pp. 1–4.

[40] S. Lahokallio, J. Kiilunen, and L. Frisk, "Performance of passive RFID tags in a high temperature cycling test," in *Proc. Electron. Syst. Integr. Technol. Conf.*, Helsinki, Finland, 2014, pp. 1–5.

[41] A. Gutierrez *et al.*, "High-frequency RFID tag survivability in harsh environments," in *Proc. IEEE Int. Conf. RFID*, Penang, Malaysia, 2013, pp. 58–65.

[42] J. Virtanen, L. Ukkonen, T. Bjorninen, A. Z. Elsherbeni, and L. Sydänheimo, "Inkjet-Printed humidity sensor for passive UHF RFID systems," *IEEE Trans. Instrum. Meas.*, vol. 60, no. 8, pp. 2768–2777, Aug. 2011.

[43] K. Chang, Y. H. Kim, Y. J. Kim, and Y. J. Yoon, "Functional antenna integrated with relative humidity sensor using synthesised polyimide for passive RFID sensing," *Electron. Lett.*, vol. 43, no. 5, pp. 259–260, Mar. 2007.

[44] S. Manzari *et al.*, "Humidity sensing by polymer-loaded UHF RFID antennas," *IEEE Sensors J.*, vol. 12, no. 9, pp. 2851–2858, Sep. 2012.

[45] K. Saarinen, T. Björninen, L. Ukkonen, and L. Frisk, "Reliability analysis of RFID tags in changing humid environment," *IEEE Trans. Compon. Packag. Manuf. Technol.*, vol. 4, no. 1, pp. 77–85, Jan. 2014.

[46] A. Hasan, R. Bhattacharyya, and S. Sarma, "Towards pervasive soil moisture sensing using RFID tag antenna-based sensors," in *Proc. IEEE Int. Conf. RFID Technol. Appl.*, Tokyo, Japan, 2015, pp. 165–170.

[47] S. Kim *et al.*, "An RFID-enabled inkjet-printed soil moisture sensor on paper for 'smart' agricultural applications," in *Proc. IEEE SENSORS*, Valencia, Spain, 2014, pp. 1507–1510.

[48] C. Bauer-Reich *et al.*, "An investigation of the viability of UHF RFID for subsurface soil sensors," in *Proc. IEEE Int. Conf. Electro/Inf. Technol.*, Milwaukee, WI, USA, 2014, pp. 577–580.

[49] J. Gao, J. Siden, and H.-E. Nilsson, "Printed electromagnetic coupler with an embedded moisture sensor for ordinary passive RFID tags," *IEEE Electron Device Lett.*, vol. 32, no. 12, pp. 1767–1769, Dec. 2011.

[50] J. Siden, X. Zeng, T. Unander, A. Koptyug, and H.-E. Nilsson, "Remote moisture sensing utilizing ordinary RFID tags," in *Proc. IEEE Sensors Conf.*, Atlanta, GA, USA, 2007, pp. 308–311.

[51] S. Prasad, S. S. Ghahfarokhi, and D. Tayari, "Impact of moisture content on RFID antenna performance for wood-log monitoring," in *Proc. 3rd RF Meas. Technol. Conf.*, Gävle, Sweden, 2011, p. 3.

[52] M. Toivonen, T. Björninen, L. Sydänheimo, L. Ukkonen, and Y. Rahmat-Samii, "Impact of moisture and washing on the performance of embroidered UHF RFID tags," *IEEE Antennas Wireless Propag. Lett.*, vol. 12, pp. 1590–1593, 2013.

[53] J. Nummela, L. Ukkonen, and L. Sydänheimo, "Passive UHF RFID tags in arctic environment," *Int. J. Commun.*, vol. 2, no. 1, pp. 135–142, 2008.

[54] E. M. Amin, R. Bhattacharyya, S. Kumar, S. Sarma, and N. C. Karmakar, "Towards low-cost resolution optimized passive UHF RFID light sensing," in *Proc. WAMICON*, Tampa, FL, USA, 2014, pp. 1–6.

[55] D. M. Dobkin and S. M. Weigand, "Environmental effects on RFID tag antennas," in *IEEE MTT S Int. Microw. Symp. Dig.*, vol. 1, Long Beach, CA, USA, 2005, pp. 135–138.

[56] A. J. Mercer *et al.*, "RFID testing and evaluation for an RF-harsh environment," in *Proc. IEEE Int. Conf. RFID Technol. Appl.*, Sitges, Spain, 2011, pp. 95–102.

[57] J. D. Griffin, G. D. Durgin, A. Haldi, and B. Kippelen, "RF Tag antenna performance on various materials using radio link budgets," *IEEE Antennas Wireless Propag. Lett.*, vol. 5, pp. 247–250, 2006.

[58] J. Alarcon, R. Saba, M. Egels, and P. Pannier, "A flexible UHF RFID tag for harsh environments," in *Proc. IEEE Int. Conf. RFID Technol. Appl.*, Nice, France, 2012, pp. 267–270.

[59] A. A. Babar, A. Z. Elsherbeni, L. Sydänheimo, and L. Ukkonen, "RFID tags for challenging environments: Flexible high-dielectric materials and ink-jet printing technology for compact platform tolerant RFID tags," *IEEE Microw. Mag.*, vol. 14, no. 5, pp. 26–35, Jul./Aug. 2013.

[60] L. M. Ni, D. Zhang, and M. R. Souryal, "RFID-based localization and tracking technologies," *IEEE Wireless Commun.*, vol. 18, no. 2, pp. 45–51, Apr. 2011.

[61] S. E. Watkins, T. M. Swift, and M. J. Molander, "RFID instrumentation in a field application," in *Proc. IEEE Region 5 Tech. Conf.*, Fayetteville, AR, USA, 2007, pp. 400–403.

[62] *EPC^{TM} Radio-Frequency Identity Protocols Generation-2 UHF RFID, Standard 2.0.1*, EPCglobal Inc., Lawrenceville, NJ, USA, Apr. 2015.

[63] *ETSI EN 302-208*, ETSI Standard 3.1.0, Feb. 2016.

[64] R. K. Yadav, J. Kishor, and R. L. Yadava, "Effects of temperature variations on microstrip antenna," *Int. J. Netw. Commun.*, vol. 3, no. 1, pp. 21–24, 2013.

[65] G. Zhang, S. Nakaoka, and Y. Kobayashi, "Millimeter wave measurements of temperature dependence of complex permittivity of dielectric plates by the cavity resonance method," in *Proc. Asia–Pac. Microw. Conf.*, vol. 3. Hong Kong, 1997, pp. 913–916.

[66] S. K. Dhawan, "Understanding effect of Teflon room temperature phase transition on coax cable delay in order to improve the measurement of TE signals of deuterated polarized targets," *IEEE Trans. Nucl. Sci.*, vol. 39, no. 5, pp. 1331–1335, Oct. 1992.

[67] J. Arbuthnott, R. Gehm, and J. Nevin, "Variation of the electrical length of coaxial transmission lines with temperature," in *Proc. Annu. Rep. Conf. Elect. Insulat.*, Washington, DC, USA, 1960, pp. 187–189.

[68] K. Czuba and D. Sikora, "Temperature stability of coaxial cables," *Acta Phys. Polonica A*, vol. 119, no. 4, pp. 553–557, Apr. 2011.

[69] D. Slack, "Minimizing temperature induced phase errors in coaxial cables," *Microw. J.*, vol. 60, no. 3, pp. 12–22, Mar. 2017.

[70] V. L. Lanza and D. B. Herrmann, "The density dependence of the dielectric constant of polyethylene," *J. Polym. Sci.*, vol. 28, no. 118, pp. 622–625, Apr. 1958.

[71] K. S. Gage and B. B. Balsley, "On the scattering and reflection mechanisms contributing to clear air radar echoes from the troposphere, stratosphere, and mesophere," *Radio Sci.*, vol. 15, no. 2, pp. 243–257, Mar./Apr. 1980.

[72] F. W. Murray, "On the computation of saturation vapor pressure," *J. Appl. Meteorol.*, vol. 6, no. 1, pp. 203–204, Feb. 1967.

[73] M. Kurri and A. Huuskonen, "Measurements of the transmission loss of a radome at different rain intensities," *J. Atmos. Ocean. Technol.*, vol. 25, no. 9, pp. 1590–1599, Sep. 2008.

[74] J. L. Salazar-Cerreño *et al.*, "A drop size distribution (DSD)-based model for evaluating the performance of wet radomes for dual-polarized radars," *J. Atmos. Ocean. Technol.*, vol. 31, pp. 2409–2430, Nov. 2014.

[75] J. T. Simpson, S. R. Hunter, and T. Aytug, "Superhydrophobic materials and coatings: A review," *Rep. Progr. Phys.*, vol. 78, no. 8, Jul. 2015, Art. no. 086501.

[76] A. Ghahremani, Q. Fu, D. Baiya, J. Simpson, and A. E. Fathy, "Performance of flexible antennas with protective super-hydrophobic coating layers at RF frequencies," in *Proc. IEEE Radio Wireless Symp.*, Austin, TX, USA, 2016, pp. 32–35.

[77] J. Niklewski, M. Fredriksson, and T. Isaksson, "Moisture content prediction of rain-exposed wood: Test and evaluation of a simple numerical model for durability applications," *Build. Environ.*, vol. 97, pp. 126–136, Feb. 2016.

[78] A. Droin, J. L. Taverdet, and J. M. Vergnaud, "Modeling the kinetics of moisture adsorption by wood," *Wood Sci. Technol.*, vol. 22, no. 1, pp. 11–20, Mar. 1988.

[79] W. L. James, "Dielectric behavior of Douglas-fir at various combinations of temperature, frequency, and moisture content," *Forest Prod. J.*, vol. 27, no. 6, pp. 44–48, 1977.

[80] R. Gonçalves *et al.*, "RFID-based wireless passive sensors utilizing cork materials," *IEEE Sensors J.*, vol. 15, no. 12, pp. 7242–7251, Dec. 2015.

[81] G. Mainsant, G. Chambon, D. Jongmans, E. Larose, and L. Baillet, "Shear-wave-velocity drop prior to clayey mass movement in laboratory flume experiments," *Eng. Geol.*, vol. 192, pp. 26–32, Jun. 2015.